

Investigating the Influence of Precursor Concentration on the Photodegradation of Methylene Blue using Biosynthesized ZnO from *Pometia pinnata* Leaf Extracts

Ari Sulisty Rini*, Yolanda Rati, Rahmi Dewi, Seliana Putri

Department of Physics, Faculty of Mathematics and Natural Sciences, University of Riau, Pekanbaru, Indonesia.

*Corresponding Author.

Received 07/06/2023, Revised 28/10/2023, Accepted 30/10/2023, Published 05/12/2023



This work is licensed under a [Creative Commons Attribution 4.0 International License](https://creativecommons.org/licenses/by/4.0/).

Abstract

The ZnO nanoparticles were synthesized at various precursor concentrations i.e. 0.05, 0.1, and 0.5 M by biosynthesis method based on *Pometia pinnata* Leaf Extracts. Initial nanoparticle concentration influenced the optical bandgap, shape, and structure of nanoparticles. The photodegradation process was carried out under UV illumination. The efficiency of MB degradation was determined by measuring the decrease in MB concentration and by analyzing the optical absorption at 663 nm recorded by UV-Vis spectroscopy. Results showed that the biosynthesized ZnO nanoparticles exhibited efficient photodegradation of MB, with a maximum degradation rate of 80% after 90 minutes of exposure to UV-C light. The study highlights the potential of *Pometia pinnata* leaf extracts as a low-cost and eco-friendly alternative for synthesizing ZnO nanoparticles for use in environmental remediation processes.

Keywords: Eco-friendly, Good absorption, Remediation, UV illumination, Zinc oxide

Introduction

Zinc oxide (ZnO) is an IIB-VIA group semiconductor with a wide bandgap energy of 3.37 eV, a high exciton energy of 60 meV, a high melting point of 2248 K, and a rapid decomposition rate over 1650 K¹. ZnO is one of the most extensively studied materials because it has interesting properties like being conductive in a wide range of light illumination and transmitting light in the visible spectrum. ZnO is widely used in various applications such as optoelectronics, cosmetics, pharmaceuticals, and photocatalysis because it is inexpensive, non-toxic, stable, and can work in the UV spectrum^{2,3}. Synthesis conditions can modify the structure and morphology of ZnO so that its physical and chemical properties change. Different preparation methods produce various ZnO shapes, such as nanobelts,

nanotubes, nanowires, nanoflowers, nanospheres, and nanorods⁴.

ZnO can be synthesized in several ways. The biosynthesis method has currently become popular in the synthesis of ZnO because it is less costly, non-toxic, eco-friendly, and requires lower temperatures than physical and chemical methods⁵. This approach employs phenolic compounds found in microbes and plant extracts as reducing agents, stabilizing agents, and capping and controlling the shape and size of nanoparticles. The utilization of microbes such as fungi, algae, bacteria, and viruses is less desirable because the process is very difficult^{6,7}. Stabilizing agents from plants were chosen because they are safer for the environment, easy to extract, and abundant in nature⁸. Furthermore, antioxidants of plants such as polyphenols, polysaccharides,

vitamins, flavonoids, tannins, alkaloids, terpenoids, and saponins have a higher content so as easier to convert metal ions to metal atoms (reductive)⁹. ZnO biosynthesis using *Musa acuminata*¹⁰, *Cinnamomum tamala*¹¹, *Prunus armeniaca*¹², and *Ananas comosus*¹³ extract has been reported previously.

Pometia pinnata which is commonly called "matoa" is a native Indonesian plant belonging to the *Sapindaceae* family. The leaves of *Pometia pinnata* contain high phenolic compounds such as flavonoids and tannins¹⁴. Therefore, *Pometia pinnata* leaves have the potential to be used in the nanoparticle biosynthesis process. Several studies have reported the use of *Pometia pinnata* leaf extract to be effective for Fe₂O₃¹⁵ and SnO₂ catalyst¹⁶. However, the utilization of *Pometia pinnata* leaf extract for synthesizing ZnO nanoparticles has not been reported.

ZnO biosynthesis is often applied to the photodegradation of pollutant wastes (toxic dyes), one of which is methylene blue. This pollutant is widely used in industry because it is cheap and dissolves quickly in water and alcohol^{17,18}. Methylene blue (C₁₆H₁₈C₁N₃S) is a very stable toxic aromatic hydrocarbon compound that is difficult to decompose naturally^{19,20}. The ability to detoxify water and increase the activity of degradation of dyes under UV light are the advantages of ZnO in the photodegradation process. Decomposition of colored

pollutants using a ZnO catalyst can reduce organic dyes thoroughly to H₂O, CO₂, and mineral acids²¹. Among the semiconductor materials, ZnO is most often applied in the photodegradation process because it is proven to have great performance.

The present study focuses on the photodegradation of methylene blue using ZnO nanoparticles biosynthesized from *Pometia pinnata* leaf extracts. One of the key parameters investigated in this study is the precursor concentration during the nanoparticle synthesis process. Previous research has demonstrated that the precursor concentration can significantly influence the properties of nanoparticles, including their size, structure, and catalytic activity²². However, the specific effect of precursor concentration on the photocatalytic efficiency of ZnO nanoparticles for methylene blue degradation remains relatively unexplored. Therefore, this study aims to systematically investigate the impact of precursor concentration on the size and morphology of the biosynthesized ZnO nanoparticles. By varying the precursor concentration, we will analyze the resulting changes in nanoparticle size and subsequently evaluate their photocatalytic performance for methylene blue degradation. The findings of this research hold the potential for enhancing the understanding of the green synthesis of ZnO nanoparticles and optimizing their efficiency in wastewater treatment applications.

Materials and Methods

Preparation of aqueous of *Pometia pinnata* leaves

Fresh leaves of *Pometia pinnata* were washed with water and dried under sunlight irradiation. A 2 g of powdered leaves were weighed into a beaker glass containing 100 ml distilled water and boiled for 10 min. It was filtered using Whatman paper for utilization in the synthesis of ZnO.

Route of Biosynthesis ZnO Nanoparticles

Approximately 10 mL of aqueous *Pometia pinnata* leaves were reacted with Zn(NO₃)₂.6H₂O solution at different concentrations; 50, 100, and 500 mol. The sample was synthesized using a microwave oven with a pH of 8 for 5 minutes. A white precipitate was centrifuged at 4000 rpm for 3 min. It was then washed with deionized water three times. The ZnO powder was obtained after drying.

Instrumentation

The crystal structure was analyzed using a Rigaku MiniFlex diffractometer ($\lambda_{\text{CuK}\alpha} = 1.541 \text{ \AA}$). Morphology was characterized using the FESEM model Quanta FEG 650 at magnification 50,000 times. The functional groups were investigated using SHIMADZU IR Prestige-21 FT-IR spectroscopy in the range of 4500 – 500 cm⁻¹. A Cary 60 spectrophotometer was used to study optical properties in the UV-Vis region.

MB Degradation Test

As much as 10 mg of ZnO powder was dissolved in 5 ppm methylene blue. It was homogenized under dark conditions for 1 h to reach adsorption-desorption equilibrium. Photodegradation was carried out under UV light ($\lambda = 237 \text{ nm}$) for 90 minutes. The solution is taken every 10 minutes to

evaluate the optical absorption. The degradation of the dye is evidenced by the loss of the methylene blue color.

Results and discussion

XRD Characterization

The X-ray diffraction pattern in Fig 1 was studied to determine the crystalline phase of biosynthesis ZnO. The XRD spectrum of the ZnO sample using *Pometia pinnata* leaf extract exhibits sharp peaks indicating high crystallinity.

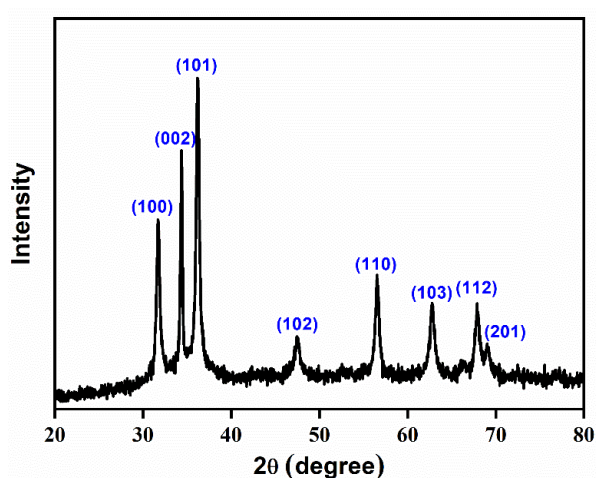


Figure 1. XRD pattern of biosynthesized ZnO.

The diffraction peaks have Miller indices (100), (002), (101), (102), (110), (103), (112), and (201) confirmed by the JCPDS of ZnO file no. 36-1451. It indicates the ZnO crystalline phase with the hexagonal wurtzite structure¹⁰. The XRD peaks of the samples all originate from ZnO crystal planes without the presence of other phase peaks. The XRD analysis indicates that the ZnO biosynthesis resulted in pure crystalline without impurities²³. The lattice parameters of the samples are obtained of $a = 3.064 \text{ \AA}$ and $c = 4.911 \text{ \AA}$. It is in accordance with the lattice parameters of the hexagonal ZnO²⁴. Table 1 presents the positions of the diffraction peaks along with the XRD parameters.

Table 1. XRD parameter of biosynthesis ZnO

hkl planes	2θ (°)	d-spacing (Å)	FWHM (°)	Crystallite size (nm)
100	31.73	2.654	0.477	17.31
002	34.37	2.455	0.263	31.58
101	36.21	2.334	0.418	20.01
102	47.49	1.802	0.750	11.57
110	56.56	1.531	0.538	16.78
103	62.80	1.393	0.678	13.73
112	67.93	1.299	0.610	15.70
201	68.98	1.281	0.882	10.92

The average distance between planes (d-spacing) is 1.844 \AA using the Bragg relation. The crystallite size is obtained by the Debye-Scherrer equation. The average crystallite size of biosynthesis ZnO samples was 17.20 nm .

FESEM Morphology

The surface morphology of ZnO biosynthesis was studied based on the FESEM photo in Fig 2. At 50,000 times magnification, it can be seen that the three samples have oval and spherical grain morphology.

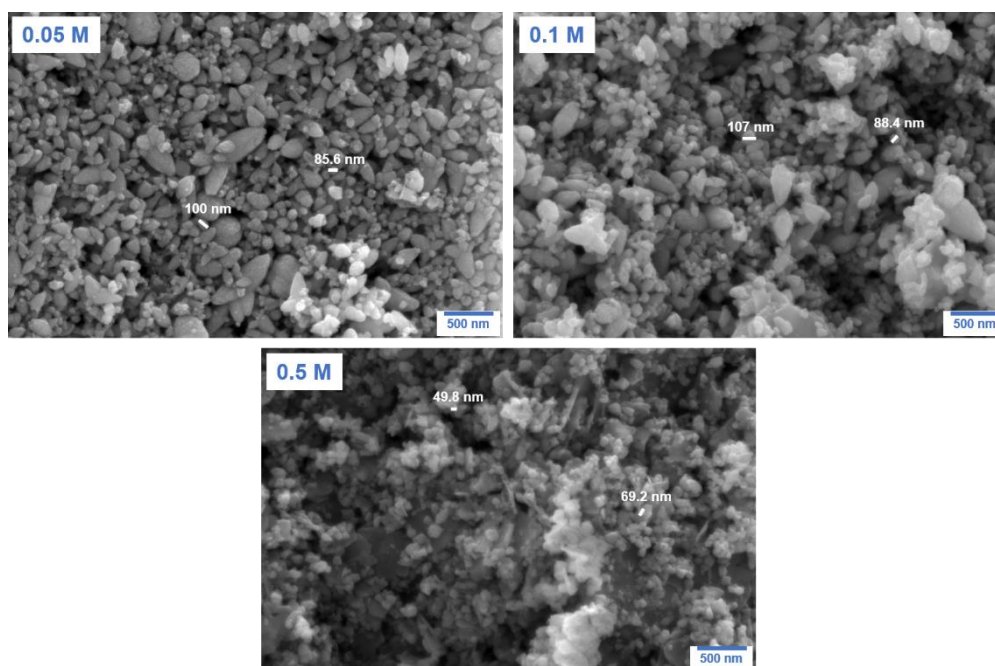


Figure 2. FESEM images of biosynthesized ZnO.

The 0.05 M sample has a uniform spherical morphology. This shows that the concentration of sample preparation affects the shape of the ZnO particles²⁵. This morphology is similar to research reported by Pai et al. synthesized ZnO using soga leaf extract (*Peltophorum pterocarpum*)⁹. The particle sizes of the 0.05 M, 0.1 M, and 0.5 M samples were 110.1, 105.2, and 62.9 nm, respectively. The high concentration can reduce the particle size. It is in line with research by Fuad et al. that prepared ZnO using the hydrothermal method²⁶.

FT-IR Characterization

FT-IR spectroscopy is a characterization to determine the bonding of sample functional groups in the infrared spectrum resulting from the incident photon molecule vibrations²⁷. The FT-IR spectrum in Fig 3 shows the first stretch at 3588.7 - 3128.67 cm^{-1} which indicates the presence of the O-H functional group. In the peak of 1610.63 cm^{-1} (amide), there is the C=O functional group which is a carboxylic acid. C-H bending vibrations are seen at around 1383.98 cm^{-1} . These peaks originated from the phytochemicals contained in the *Pometia pinnata* leaf extract. The determination of functional group bond is determined by reference²⁸.

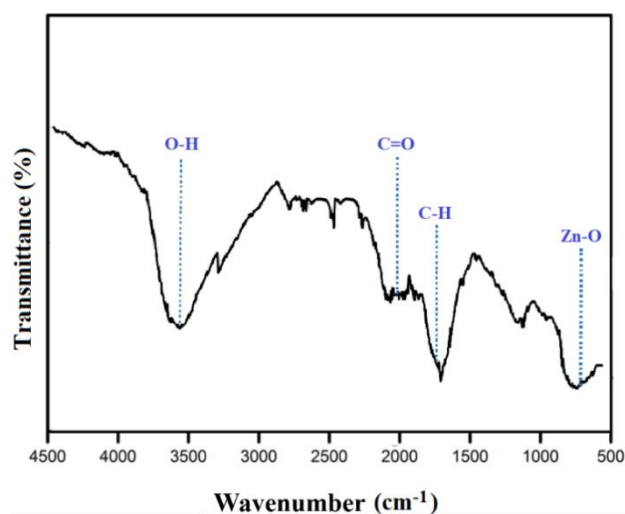


Figure 3. FT-IR spectrum of biosynthesized ZnO.

The ZnO stretching band phase was observed at around 465.83 cm^{-1} . It confirms the presence of ZnO in biosynthesis samples⁸. Thus, the formation of the ZnO structure with *Pometia pinnata* leaf extract has been achieved due to the interaction of oxygen with other functional groups present in the extract. It is in accordance with a previous research report by Candogan et al. using neem (*Azadirachta indica*) leaf extract²⁹.

UV-Vis Analysis

The optical properties of the ZnO samples were analyzed from the UV-Vis absorbance spectrum.

UV-Vis spectroscopy was used to identify the formation of biosynthesized ZnO. The absorbance spectrum of the ZnO samples using *Pometia pinnata* leaves can be seen in Fig 4a. Strong absorption occurs at 250-390 nm, while weak absorption occurs at 390-750 nm. Similar studies were reported previously on the synthesis of ZnO using the leaf

extract of *Corriandrum sativum*⁸. The absorption peaks of all samples with different concentrations of 0.05 M, 0.1 M, and 0.5 M are at 375 nm, 369 nm, and 368 nm, respectively. It shows that ZnO has a high absorption in the UV region so it is very good to be applied as a photocatalyst³⁰.

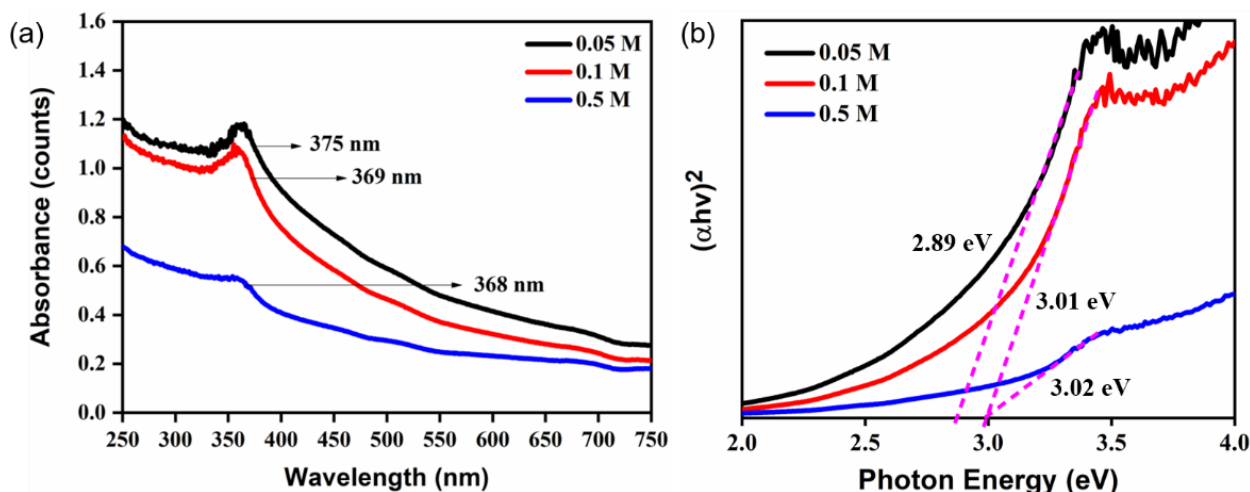


Figure 4. (a) Absorbance spectrum and (b) Bandgap curve of biosynthesized ZnO.

Fig 4b shows the band gap energy of biosynthesized ZnO. Bandgap energy was obtained by extrapolating the absorbance spectra using the Tauc plot method. ZnO samples with concentrations of 0.05 M, 0.1 M, and 0.5 M have band gap energies of 2.89 eV, 3.01 eV, and 3.02 eV respectively. The gap energy difference is believed due to a reduction in the number of vacancies between oxygen and zinc³¹. The low band gap energy obtained plays an

important role in the excitation of electrons in applications that utilize light.

Degradation MB Analysis

Biosynthesis ZnO catalyst has been effective for the photodegradation of methylene blue under UV illumination for 90 minutes. It was observed from the color change of methylene blue to almost colorless. The degradation process was evaluated by absorption at 663 nm¹⁸, which can be seen in Fig 5a.

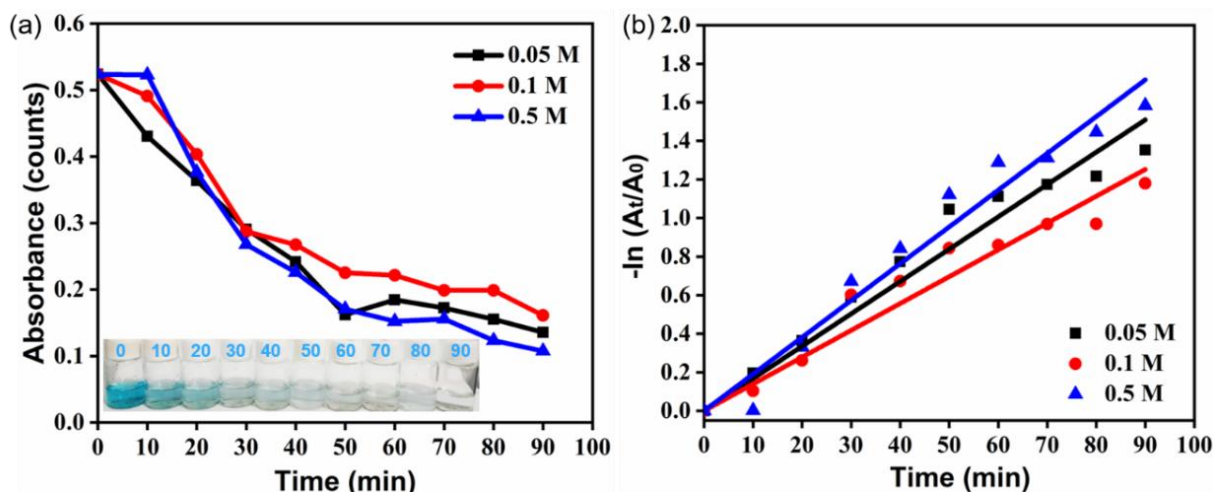


Figure 5. (a) A_t/A_0 curve and (b) $\ln(A_t/A_0)$ curve of biosynthesized ZnO.

The decrease in the absorption curve indicates that the concentration of methylene blue reduces due to the ZnO catalyst¹⁰. All biosynthesis ZnO samples with different concentrations exhibited almost the same reduction in absorption. The reduction in methylene blue concentration for 90 minutes for 0.05 M, 0.1 M, and 0.5 M samples was 74%, 70%, and 80%, respectively. In addition, the UV light source is also influential in this process due to ZnO exhibits a strong absorption in the UV region⁹. Photodegradation occurs due to charge separation in the ZnO structure due to UV irradiation. The excited electrons will leave the hole. Both charge carriers react with water and oxygen to produce hydroxyl radicals and superoxide radicals thereby degrading the dye to CO₂ dan H₂O²¹.

Fig 5b presents the $-\ln(A_t/A_0)$ versus time curves to study the kinetics of the photodegradation reaction rate of methylene blue. The reaction rate constant was determined using by following equation³²:

Conclusion

It has successfully synthesized ZnO using *Pometia pinnata* leaf extract with an eco-friendly and inexpensive method for the photodegradation of methylene blue. Some of the characteristics obtained are as follows. ZnO has high crystallinity of the hexagonal wurtzite structure, oval and spherical grain morphology, and the ZnO stretching band phase was confirmed at 465.83 cm⁻¹ in the FTIR

Acknowledgment

This work is funded by the Ministry of Education, Culture, Research, and Technology of the Republic of Indonesia year 2023 research grant. The authors

Author's Declaration

- Conflicts of Interest: None.
- We hereby confirm that all the Figures and Tables in the manuscript are ours. Besides, the Figures and images, which are not ours, have been given

Author's Contribution

A. S. R. designed the study and concept. A. S. R. and Y.R. analyzed data and interpretation. Y. R. and R.

References

1. Asadian M. Thermodynamic Analysis of ZnO Crystal

$$-\ln\left(\frac{A_t}{A_0}\right) = kt \quad 1$$

Where A_t and A_0 are post and initial irradiation absorbance of MB at 663 nm, t is time irradiation, and k is the rate constant of the reduction reaction. The 0.05 M, 0.1 M, and 0.5 M ZnO samples each had reaction rates of 0.0168 min⁻¹, 0.0139 min⁻¹, and 0.0191 min⁻¹. The high value of the reaction rate indicates the amount of pollutant that reacts to a given ZnO sample. Also, the increase in the reaction rate indicates that methylene blue is rapidly degraded. Previous research reported that photodegradation of methylene blue occurred at a reaction rate of 0.00402 min⁻¹ using a SnO₂ catalyst based on *Pometia pinnata* leaf extract¹⁶. It proved that biosynthesis of ZnO using *Pometia pinnata* leaf extract has excellent of photodegradation of methylene blue.

spectrum. Also, good absorption in the UV region. For the photodegradation process under UV light, it was shown that the biosynthesized ZnO nanoparticles exhibited an efficient degradation rate of 80%. The research concludes that ZnO possesses the potential to be used in aqueous environment remediation processes.

also would like to thank the Lembaga Penelitian dan Pengabdian (University of Riau), for supporting this research.

the permission for re-publication attached with the manuscript.

- Ethical Clearance: The project was approved by the local ethical committee at University of Riau.

D performed revision and proofreading. A. S. R. and S.P. conducted the experiments and drafting the MS.

Growth from the Melt. J Cryst Process Technol. 2013

- July; 3(3): 75–80.
<http://doi.org/10.4236/jcpt.2013.33012>
- Sulciute A, Nishimura K, Gilshtein E, Cesano F, Viscardi G, Nasibulin AG, et al. ZnO Nanostructures Application in Electrochemistry: Influence of Morphology. *J Phys Chem C*. 2021 January; 125(2): 1472–1482.
<https://pubs.acs.org/doi/10.1021/acs.jpcc.0c08459>
 - Khadayeir AA, Wannas AH, Yousif FH. Effect of Applying Cold Plasma on Structural, Antibacterial and Self Cleaning Properties of α -Fe₂O₃ (HEMATITE) Thin Film. *Emerg Sci J*. 2022; 6(1): 75-85.
<https://doi.org/10.28991/ESJ-2022-06-01-06>
 - Aranda A, Landers R, Carnelli P, Candal R, Alarcón H, Rodríguez J. Influence of silver electrochemically deposited onto zinc oxide seed nanoparticles on the photoelectrochemical performance of zinc oxide nanorod films. *Nanomater. Nanotechnol*. 2019 May; 9: 1-9. <https://doi.org/10.1177/184798041984436>
 - Cruz DM, Mostafavi E, Crua AV, Barabadi H, Shah V, Diaz JLC, et al. Green nanotechnology-based zinc oxide (ZnO) nanomaterials for biomedical applications: A review. *J Phys Mater*. 2020 May; 3(3): 034005. <https://doi.org/10.1088/2515-7639/ab8186>
 - Kalpana VN, Kataru BAS, Sravani N, Vigneshwari T, Panneerselvam A, Rajeswari VD. Biosynthesis of zinc oxide nanoparticles using culture filtrates of *Aspergillus niger*: Antimicrobial textiles and dye degradation studies. *OpenNano*. 2018 June; 3: 48–55.
<https://doi.org/10.1016/j.onano.2018.06.001>
 - Perrot C, Ferguson HJ, Mulholland M, Brown A, Buckley C, Humphrey J, et al. Rendered Services and Dysservices of Dairy Farming to the Territories: A Bottom-up Approach in European Atlantic Area. *J Hum Earth Fut*. 2022; 3(3): 396-402.
<https://doi.org/10.28991/HEF-2022-03-03-010>
 - Jalab J, Abdelwahed W, Kitaz A, Al-Kayali R. Green synthesis of silver nanoparticles using aqueous extract of *Acacia cyanophylla* and its antibacterial activity. *Heliyon*. 2021 September; 7(9): e08033.
<https://doi.org/10.1016/j.heliyon.2021.e08033>
 - Xu J, Huang Y, Zhu S, Abbes N, Jing X, Zhang L. A review of the green synthesis of ZnO nanoparticles using plant extracts and their prospects for application in antibacterial textiles. *J Eng Fiber Fabr*. 2021 September; 16: 1-14.
<https://doi.org/10.1177/1558925021104624>
 - Abdullah FH, Bakar NHHA, Bakar MA. Low temperature biosynthesis of crystalline zinc oxide nanoparticles from *Musa acuminata* peel extract for visible-light degradation of methylene blue. *Optik*. 2020 March; 206: 164279.
<https://doi.org/10.1016/j.ijleo.2020.164279>
 - Narath S, Koroth SK, Shankar SS, George B, Mutta S, Waclawek S, et al. *Cinnamomum tamala* leaf extract stabilized zinc oxide nanoparticles: A promising photocatalyst for methylene blue degradation. *Nanomaterials*. 2021 June; 11(6): 1558.
<https://doi.org/10.3390/nano11061558>
 - Abdullah SM, Al-hamdani AAS, Al-zubaidi LA. Water Treatment Using Zinc Nanoparticles and Apricot Plant Extracts from Organic and Inorganic Pollution. *Baghdad. Sci J*. 2023 May.
<https://doi.org/10.21123/bsj.2023.7952>
 - Rini AS, Rahayu SD, Hamzah Y, Linda TM, Rati Y. Effect of pH on the morphology and microstructure of ZnO synthesized using *anasan comosus* peel extract. *J Phys Conf Ser*. 2021; 2019(1): 012100.
<https://doi.org/10.1088/1742-6596/2019/1/012100>
 - Munirah Malaka R, Maruddin F. Antioxidant activity of milk pasteurization by addition of Matoa leaf extract (*Pometia pinnata*). *IOP Conf Ser Earth Environ Sci*. 2020; 492(1): 012046. <https://doi.org/10.1088/1755-1315/492/1/012046>
 - Syarifah S, Imawan C, Handayani W, Djuhana D. Biosynthesis of ferric oxide nanoparticles using *Pometia pinnata* J. R. Frost. & G. Forst. leaves water extract. *AIP Conf Proc*. 2018 October; 2023(1): 020054. <https://doi.org/10.1063/1.5064051>
 - Sujatmiko F, Sahroni I, Fadillah G, Fatimah I. Visible light-responsive photocatalyst of SnO₂/rGO prepared using *Pometia pinnata* leaf extract. *Open Chem*. 2021; 19(1): 174-183. <https://doi.org/10.1515/chem-2020-0117L>
 - Youcef LD, Belaroui LS, Galindo AL. Adsorption of a cationic methylene blue dye on an Algerian *palygorskite*. *Appl Clay Sci*. 2019 October; 179: 105145. <https://doi.org/10.1016/j.clay.2019.105145>
 - Ratnawati R, Wulandari R, Kumoro AC, Hadiyanto H. Response surface methodology for formulating PVA/starch/lignin biodegradable plastic. *Emerg Sci J*. 2022; 6(2): 238-255. <https://doi.org/10.28991/ESJ-2022-06-02-03>
 - Yao X, Ji L, Guo J, Ge S, Lu W, Cai L, et al. Magnetic activated biochar nanocomposites derived from wakame and its application in methylene blue adsorption. *Bioresour Technol*. 2020 April; 302: 122842.
<https://doi.org/10.1016/j.biortech.2020.122842>
 - Wahlström N, Steinhagen S, Toth G, Pavia H, Edlund U. Ulvan dialdehyde-gelatin hydrogels for removal of heavy metals and methylene blue from aqueous solution. *Carbohydr Polym*. 2020 December; 249: 116841.
<https://doi.org/10.1016/j.carbpol.2020.116841>
 - Lee KM, Lai CW, Ngai KS, Juan JC. Recent developments of zinc oxide based photocatalyst in water treatment technology: A review. *Water Res*. 2016 January; 88: 428–448.
<https://doi.org/10.1016/j.watres.2015.09.045>
 - Jihoon PC, Park KS Lee, Su-Jeong Suh. Effect of NaOH and precursor concentration on size and magnetic properties of FeCo nanoparticles synthesized using the polyol method. *AIP Adv*. 2020; 10: 115220.
<https://doi.org/10.1063/5.0024622>
 - Qian Y, Wei H, Dong J, Yunzhe D, Fang X, Wenhui

- Z, et al. Fabrication of urchin-like ZnO-MXene nanocomposites for high-performance electromagnetic absorption. *Ceram Int.* 2017; 43(14): 10757-10762. <https://doi.org/10.1016/J.CERAMINT.2017.05.082>
24. Perillo PM, Atia MN, Rodríguez DF. Studies on the growth control of ZnO nanostructures synthesized by the chemical method. *Rev Mater.* 2018; 23(2): 1-7. <https://doi.org/10.1590/S1517-707620180002.0467>
25. Ridwan M, Fauzia V, Roza L. Synthesis and characterization of ZnO nanorods prepared using microwave-assisted hydrothermal method. *IOP Conf Ser Mater Sci Eng.* 2019; 496(1): 012018. <https://doi.org/10.1088/1757-899X/496/1/012018>
26. Fakhari S, Jamzad M, Fard HK. Green synthesis of zinc oxide nanoparticles: a comparison. *Green Chem Lett Rev.* 2019 January; 12(1): 19–24. <https://doi.org/10.1080/17518253.2018.1547925>
27. Fakayode SO, Baker GA, Bwambok DK, Bhawawet N, Elzey B, Siraj N, et al. Molecular (Raman, NIR, and FTIR) spectroscopy and multivariate analysis in consumable products analysis. *Appl Spectrosc Rev.* 2020; 55(8): 647–723. <https://doi.org/10.1080/05704928.2019.1631176>
28. Bužarovska A, Dinescu S, Lazar A D, Serban M, Pircalabioru G G, Costache M. et al. Materials Science & Engineering C Nanocomposite foams based on flexible biobased thermoplastic polyurethane and ZnO nanoparticles as potential wound dressing materials. *Mat Sci Eng C.* 2019 November; 104: 109893. <https://doi.org/10.1016/j.msec.2019.109893>
29. Candogan K, Altuntas EG, İğci N. Authentication and Quality Assessment of Meat Products by Fourier-Transform Infrared (FTIR) Spectroscopy. *Food Eng Rev.* 2020 September; 13(1): 66-91. <https://doi.org/10.1007/s12393-020-09251-y>
30. Chowdhury MIH, Hossain MS, Azad MAS, Islam MZ, Dewan MA. Photocatalytic Degradation of Methyl Orange Under UV Using ZnO as Catalyst. *Int J Sci Eng Res.* 2018 June; 9(6): 1646–1649. <https://doi.org/10.14299/ijser.2018.06>
31. Fuad A, Fibriyanti AA, Subakti, Mufti N, Taufiq A. Effect of Precursor Concentration Ratio on The Crystal Structure, Morphology, and Band Gap of ZnO Nanorods. *IOP Conf Ser Mater Sci Eng.* 2017 May; 202(1): 012074. <https://doi.org/10.1088/1757-899X/202/1/012074>
32. Ahammed KR, Ashaduzzaman M, Paul SC, Nath MR, Bhowmik S, Saha O, et al. Microwave assisted synthesis of zinc oxide (ZnO) nanoparticles in a noble approach: utilization for antibacterial and photocatalytic activity. *SN Appl Sci.* 2020 April; 2(5): 1–14. <https://doi.org/10.1007/s42452-020-2762-8>

دراسة تأثير تركيز السلائف على التحلل الضوئي للميثيلين الأزرق باستخدام أكسيد الزنك الحيوي من مستخلصات أوراق نبات البوميتيا بيناتا

آري سوليسيتو ريني ، يولاندا راتي ، رحمي ديوي ، سيليانا بوتري

قسم الفيزياء ، كلية الرياضيات والعلوم الطبيعية ، جامعة رياو ، بيكانبارو ، إندونيسيا

الخلاصة

تم تصنيع جسيمات أكسيد الزنك النانوية بتركيزات مختلفة من السلائف، مثل 0.05 و 0.1 و 0.5 مولار باستخدام طريقة التخليق الحيوي المعتمدة على مستخلصات أوراق نبات البوميتيا بيناتا. أثر التركيز الأولي للجسيمات النانوية على فجوة النطاق الضوئية وشكل وبنية الجسيمات النانوية. تم تنفيذ عملية التحلل الضوئي تحت إضاءة الأشعة فوق البنفسجية. تم تحديد كفاءة تحلل بروميد الميثيل عن طريق قياس الانخفاض في تركيز بروميد الميثيل وعن طريق تحليل الامتصاص البصري عند 663 نانومتر المسجل بواسطة التحليل الطيفي للأشعة فوق البنفسجية. أظهرت النتائج أن جسيمات أكسيد الزنك النانوية المُصنَّعة حيويًا أظهرت تحللًا ضوئيًا فعالاً لـ MB، مع معدل تحلل أقصى يبلغ 80% بعد 90 دقيقة من التعرض للأشعة فوق البنفسجية. تسلط الدراسة الضوء على إمكانات مستخلصات أوراق البوميتيا بيناتا كبديل منخفض التكلفة وصادق للبيئة لتصنيع جزيئات ZnO النانوية لاستخدامها في عمليات المعالجة البيئية.

الكلمات المفتاحية: صديقة للبيئة، امتصاص جيد، معالجة، إضاءة بالأشعة فوق البنفسجية، أكسيد الزنك